

Electronic Supplementary Information to "Stressing the differences in alizarin and purpurin dyes through UV-visible light absorption and ^1H -NMR spectroscopies"

Roger-Charles Tissier,^a Baptiste Rigaud,^b Pierre Thureau,^a Miquel Huix-Rotllant,^a Maguy Jaber,^b
and Nicolas Ferré*^a

^a Aix-Marseille Univ, CNRS, Institut Chimie Radicalaire, Marseille, France. E-mail: nicolas.ferre@univ-amu.fr

^b Sorbonne Université, Laboratoire d'Archéologie Moléculaire et Structurale, Paris, France.

Contents

1	9,10-anthraquinone	2
2	Alizarin	4
3	Purpurin	8
4	Intensity borrowing hypothesis	10
5	Purpurin impurity	17

List of Figures

S1	9,10-anthraquinone computed UV-visible spectrum	2
S2	Alizarin tautomers	5
S3	Alizarin normal modes	6
S4	Alizarin NTOs	7
S5	Purpurin tautomers	8
S6	Purpurin normal modes	9
S7	Purpurin NTOs	9
S8	9,10-anthraquinone excitation energy curves	10
S9	Potential energy surface cuts along b_{1u} modes of 9,10-anthraquinone at the S_0 minimum.	11
S10	Potential energy surface cuts along b_{2u} modes of 9,10-anthraquinone at the S_0 minimum.	12
S11	Evolution of the S_4 diabatic population in a linear vibronic coupling model of S_4 and S_5 expanded in the coupling modes 17, 30 and 53 of b_{2u} symmetry.	13
S12	Alizarin excitation energy curves	14
S13	Potential energy surface cuts along a'' modes of alizarin at the S_0 minimum.	15
S14	(continue) figure S13	16
S15	Purpurin ESI-MS spectrum	17
S16	Purpurin ^{13}C -NMR spectrum	18

List of Tables

S1	9,10-anthraquinone vertical transition analysis	3
S2	Alizarin tautomer free energies	4
S3	Alizarin chemical shifts	4
S4	Purpurin tautomer free energies	8

1 9,10-anthraquinone

Six singlet-to-singlet vertical excitations have been considered in the computation of 9,10-anthraquinone UV-visible absorption spectrum. Their properties (energy differences, oscillator strengths, natural transition orbitals) are summarized in Table S1. The details of each contribution of the electronic transition to the total spectra are represented in Fig. S1.

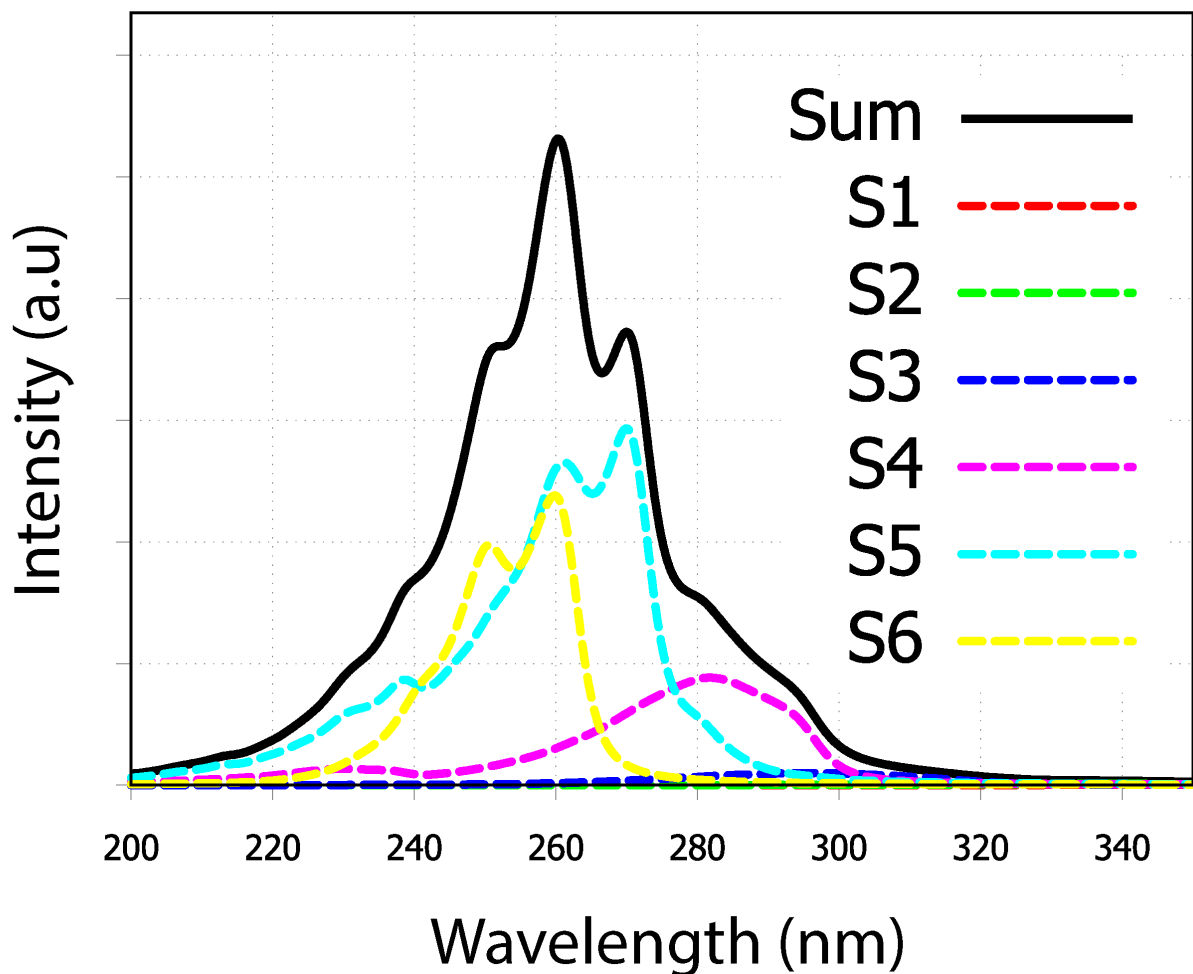


Figure S1: Contribution of each electronic transition (from $S_0 \rightarrow S_1$ to $S_0 \rightarrow S_6$) to the total spectrum (denoted as Sum). The first three transitions are represented but their relative intensities are too low to be visible in the graph.

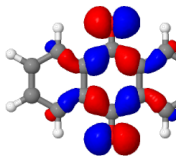
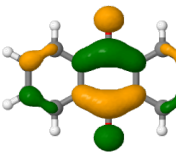
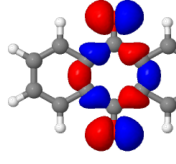
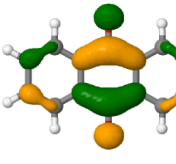
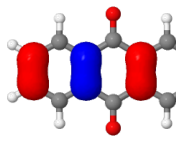
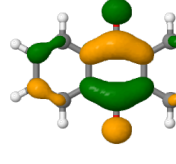
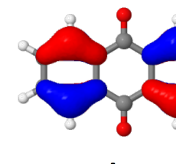
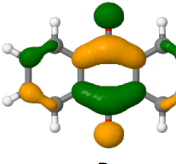
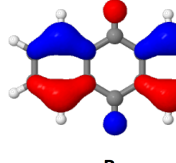
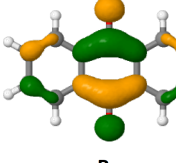
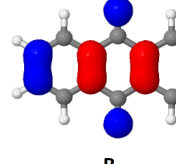
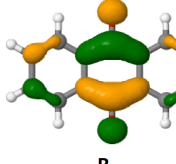
Transition	Vertical transition energy (eV)	Vertical transition wavelength (nm)	Oscillator strength	NTO weight	Irreducible representation of the transition	φ_1 NTO hole orbital (irreducible representation)	φ_2 NTO particle orbital (irreducible representation)
S_1	3.4	369.3	-	0.89	B_{1g}		
						$\langle \varphi_1 x_i \varphi_2 \rangle (i=1,2,3)$	B_{2u}
S_2	3.6	342.7	-	0.81	A_u		
						$\langle \varphi_1 x_i \varphi_2 \rangle (i=1,2,3)$	B_{3g}
S_3	4.1	299.2	-	0.97	B_{3g}		
						$\langle \varphi_1 x_i \varphi_2 \rangle (i=1,2,3)$	A_u
S_4	4.3	286.7	0.2	0.88	B_{2u}		
						$\langle \varphi_1 x_i \varphi_2 \rangle (i=1,2,3)$	B_{1g}
S_5	4.4	283.4	-	0.89	A_g		
						$\langle \varphi_1 x_i \varphi_2 \rangle (i=1,2,3)$	B_{3u}
S_6	5.0	249.2	0.3	0.91	B_{1u}		
						$\langle \varphi_1 x_i \varphi_2 \rangle (i=1,2,3)$	B_{2g}

Table S1: Six lowest vertical transitions of 9,10-anthraquinone with their corresponding energies (in eV and nm), oscillator strengths, Natural Transition Orbital (NTO) weights, NTOs and their associated symmetries in the D_{2h} point group. $\langle \varphi_1 | x_i | \varphi_2 \rangle (i = 1, 2, 3)$ reports the symmetry of each of the 3 integrals entering the corresponding vertical transition dipole moment.

2 Alizarin

Alizarin (dye content 97%) was purchased from Sigma-Aldrich (CAS number: 72-48-0).

Free energy calculations have been performed at the ω B97xD/6-31+G* level of theory, together with the Polarizable Continuum Model (PCM) for water or acetone, on all tautomers represented in Figure S2. The presence of rotamers, especially the ones involving the proton H-2, has also been considered. In the absence of noticeable effects, they will not be discussed further. While a recent work [Study of natural anthraquinone colorants by EPR and UV/vis spectroscopy, Machatová et al, Dyes and Pigments 132 (2016) 79, <https://doi.org/10.1016/j.dyepig.2016.04.046>] suggests a probable equilibrium between deprotonated alizarin tautomers, our calculations show this is not true in the case of fully protonated alizarin: only the most stable tautomer (Tautomer0) can be retained.

	Tautomer 0	Tautomer 1	Tautomer 2	Tautomer 3	Tautomer 4	Tautomer 5
Solvent = acetone	0.0	7.6	17.9	16.9	23.6	15.5
Solvent = water	0.0	7.6	17.4	16.5	23.2	15.2

Table S2: Alizarin tautomer relative free energies in kcal/mol.

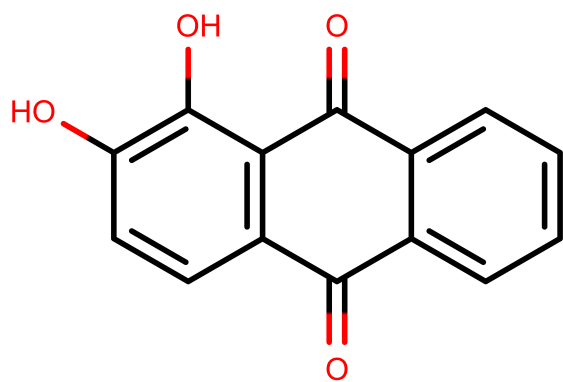
The calculation of ^1H NMR chemical shifts of **Tautomer 0** to **Tautomer 5** has been performed using a cluster (solute + a few solvent molecules) approach (ω B97xD/6-311+G(2d,p) embedded in an electrostatic continuum (PCM $\epsilon=20.493$ corresponding to acetone)). A few explicit solvent molecules have been placed close to the hydroxyl moieties, hence favoring inter-molecular hydrogen bonds. In the case of Tautomer5, no explicit solvent has been used. The results are summarized in Table S3.

	Exp	Tautomer 0	Tautomer 2	Tautomer 3	Tautomer 4	Tautomer 5
n_{solv}		2	2	2	2	0
H-1	12.82	10.84	14.74	14.39	14.45	3.87
H-2	9.91	12.76	11.49	10.16	14.29	14.53
H-3	7.34	7.64	6.68	6.62	6.82	3.87
H-4	7.99	8.28	8.67	8.90	8.43	7.92
H-5	8.32	8.80	8.22	8.36	8.82	8.89
H-6	7.78	8.31	8.18	8.19	8.47	8.38
H-7	7.97	8.28	8.16	8.17	8.22	8.38
H-8	8.27	8.85	8.97	8.00	8.92	8.95

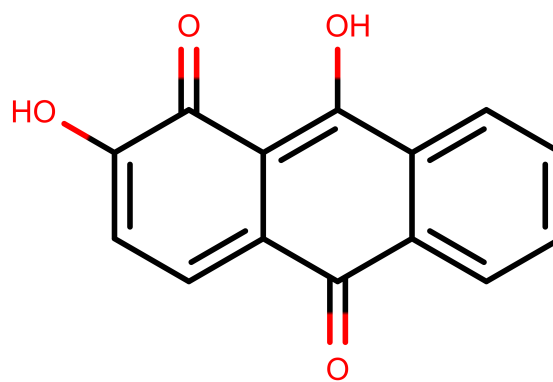
Table S3: Experimental and calculated ^1H chemical shifts (in ppm) of alizarin selected tautomers at ω B97xD/6-311+G(2d,p) PCM(solvent=acetone) level of theory. The number (n_{solv}) of explicit solvent molecules is indicated in the second row. Note that the geometry optimization of **Tautomer 1** using the 6-311++G(2d,p) basis set results in a final structure which corresponds to **Tautomer 0**, hence **Tautomer 1** does not exist at the considered level of theory.

Overall, we find that **Tautomer 0** chemical shifts agree well with the experimental ones. Together with the free energy differences reported above, these results confirm that only **Tautomer 0** needs to be considered. Solvent deuterium can exchange with alizarin hydroxyl hydrogen atoms. For the sake of completeness, we have also explored the effect of deuterated molecules on the chemical shifts. No particular effect can be noticed.

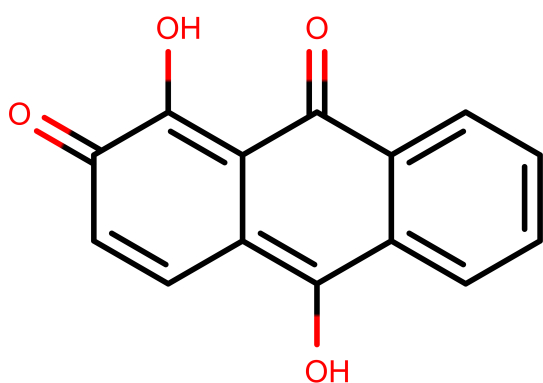
As mentioned in the main text, using the AH—FCHT scheme, several vibronic couplings contribute to increase the intensity of the $S_0 \rightarrow S_2$ vertical transition, which eventually turns to be as intense as the $S_0 \rightarrow S_1$ one. The displacement vectors associated to the normal modes coupled with the $S_0 \rightarrow S_2$ electronic transition are reported in Figure S3. Alizarin NTOs are provided for both the $S_0 \rightarrow S_1$ and $S_0 \rightarrow S_1$ transitions in Figure S4.



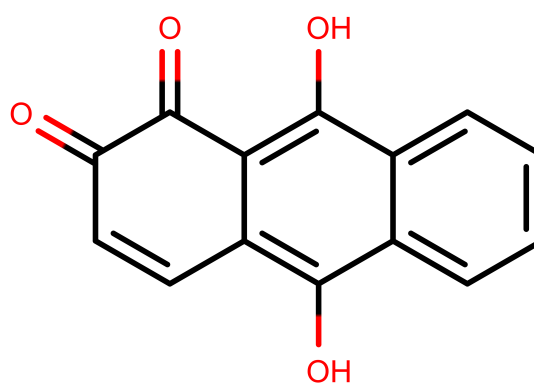
Tautomer 0



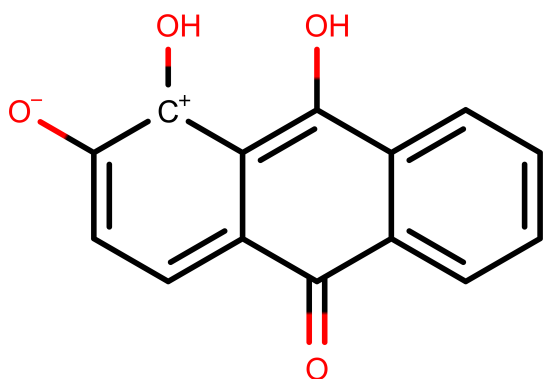
Tautomer 1



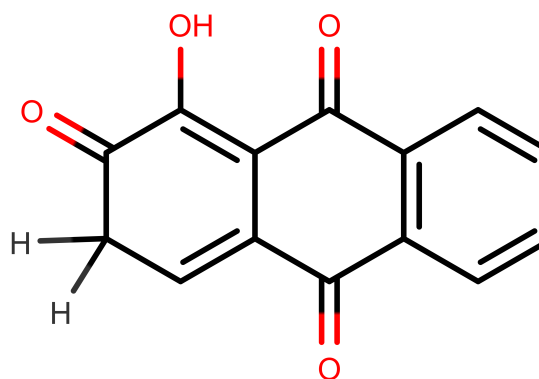
Tautomer 2



Tautomer 3



Tautomer 4



Tautomer 5

Figure S2: Structures of the alizarin tautomers considered in this work. It should be noted that several rotamers also exist but are not represented here.

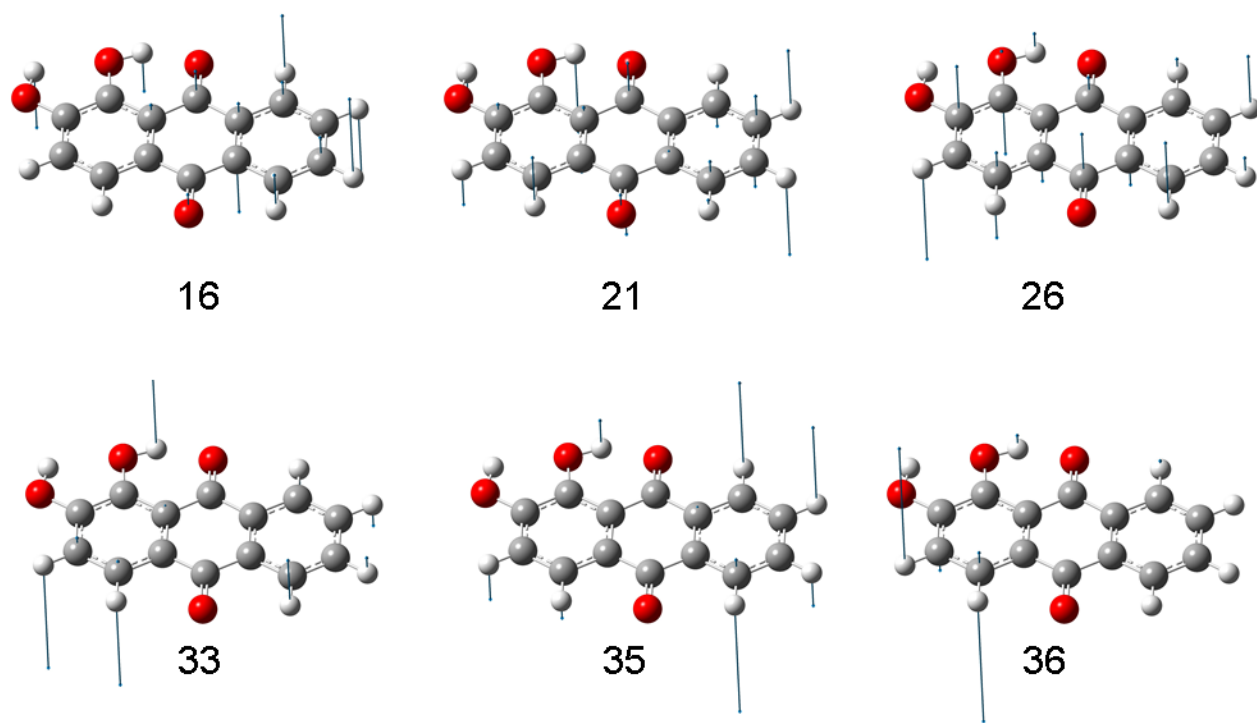
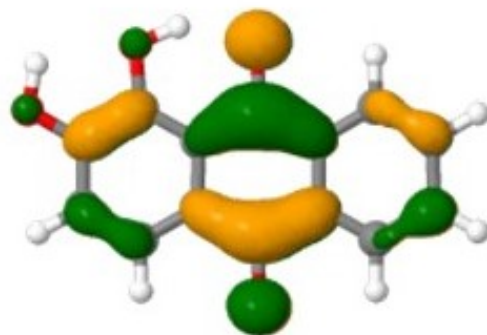
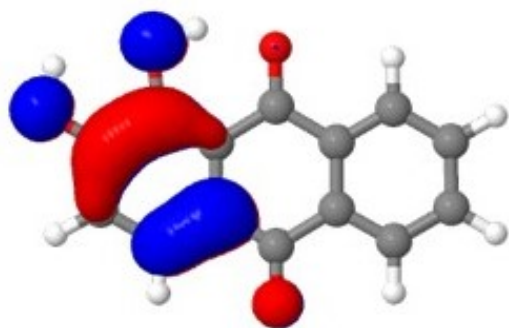


Figure S3: Normal modes coupled to the $S_0 \rightarrow S_1$ electronic transition in alizarin. The associated couplings are 2851, 4723, 1040, 7280, 1131 and 1629 a.u, respectively.

a)



b)

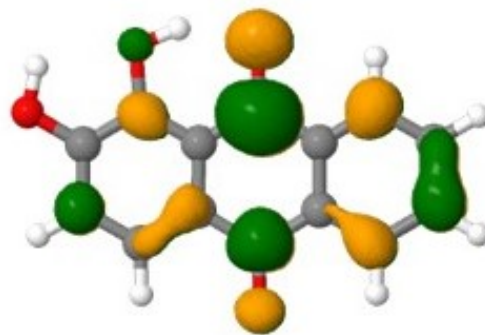
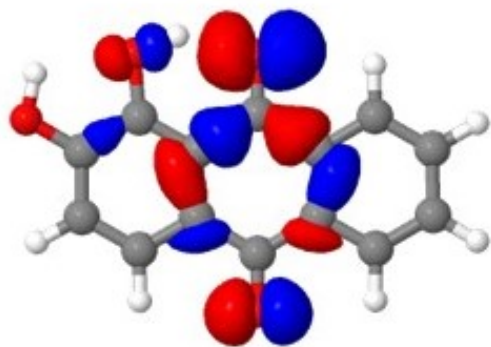
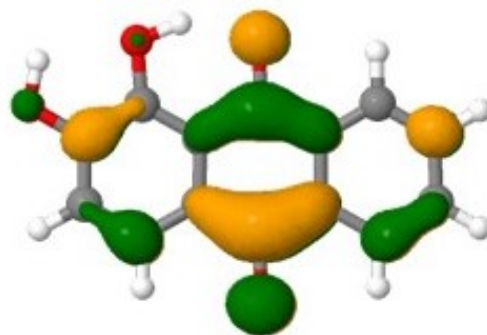
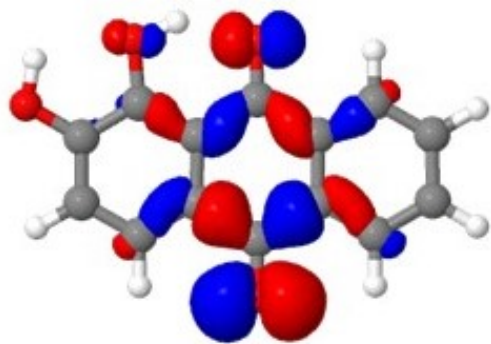


Figure S4: NTOs of $S_0 \rightarrow S_1$ (a) and $S_0 \rightarrow S_2$ (b) electronic transition: hole(left)/electron(right) orbitals.

3 Purpurin

Purpurin (dye content 90%) was purchased from Sigma-Aldrich (CAS number: 81-54-9).

Considering the neutral form of purpurin, free energy calculations have been performed at ω B97xd/6-31+G* level of theory using PCM for water or acetone solvents on a large ensemble of possible tautomers. Nevertheless, only one is energetically accessible at room temperature. Some of these tautomers are represented in Figure S5. Similarly to alizarin, purpurin rotamers have been considered, however no noticeable effect is found.

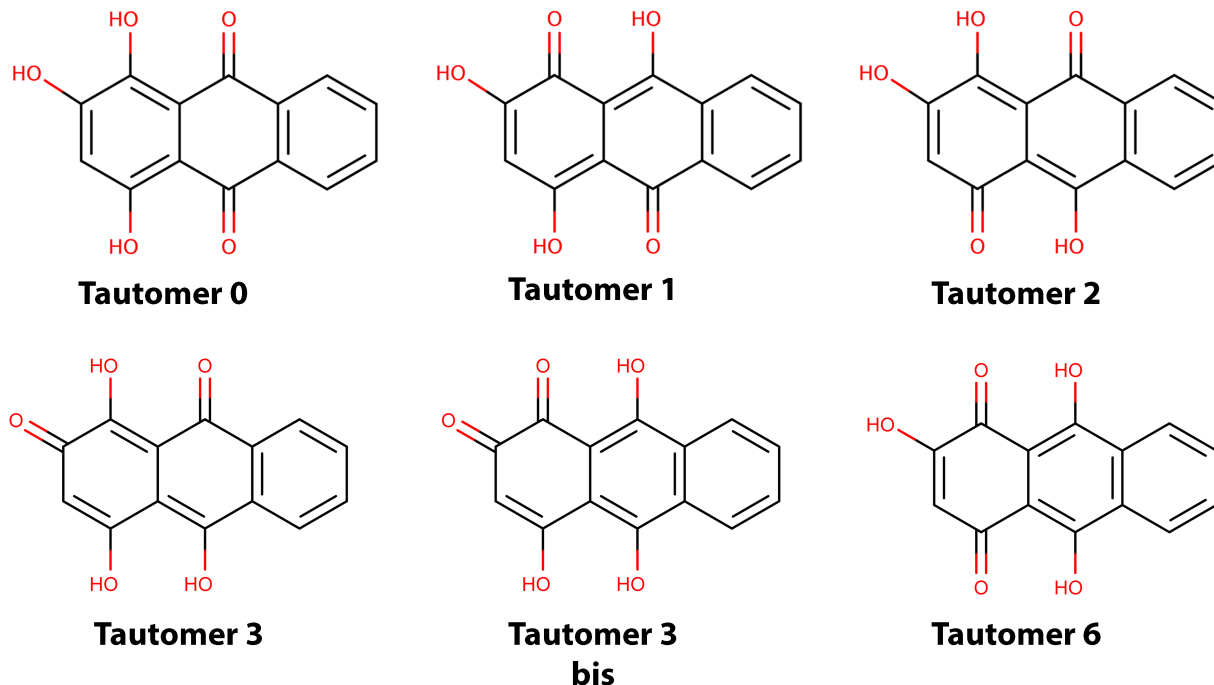


Figure S5: Structures of neutral purpurin tautomers considered in this work.

	Tautomer 0	Tautomer 1	Tautomer 2	Tautomer 3	Tautomer 3bis	Tautomer 6
Solvent = acetone	0.0	8.03	7.87	-	-	-
Solvent = water	0.0	7.9	7.7	18.5	13.5	3.5

Table S4: Purpurin tautomer relative free energies in kcal/mol.

Hereafter, we report the most important normal modes coupled to the purpurin $S_0 \rightarrow S_1$ electronic transition. Their corresponding displacements are restricted to the molecule principal plane (Figure S6).

The NTOs analysis performed on the $S_0 \rightarrow S_1$ and $S_0 \rightarrow S_1$ electronic transition of purpurin confirms the $\pi \rightarrow \pi^*$ character of the first one and the $n \rightarrow \pi^*$ of the second one.

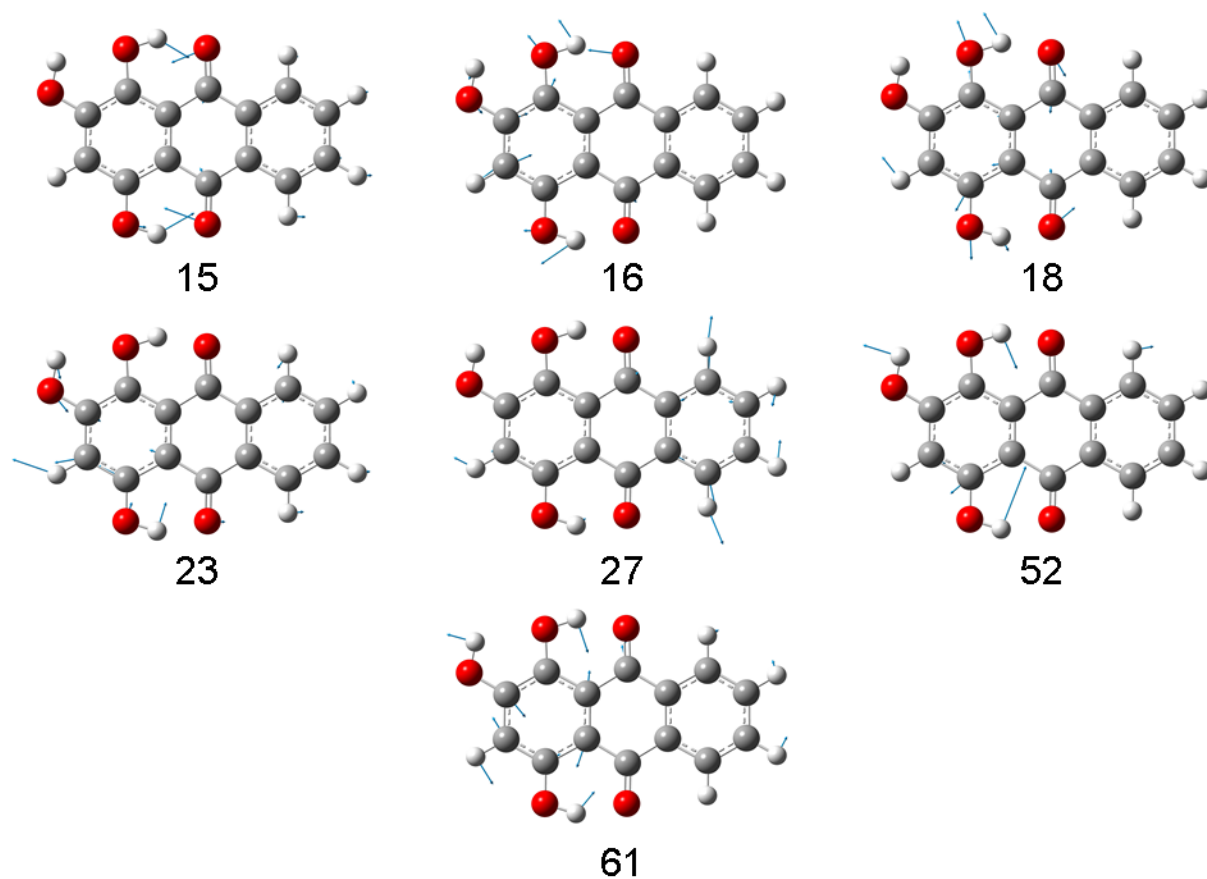


Figure S6: Normal modes coupled to the $S_0 \rightarrow S_1$ electronic transition of purpurin.

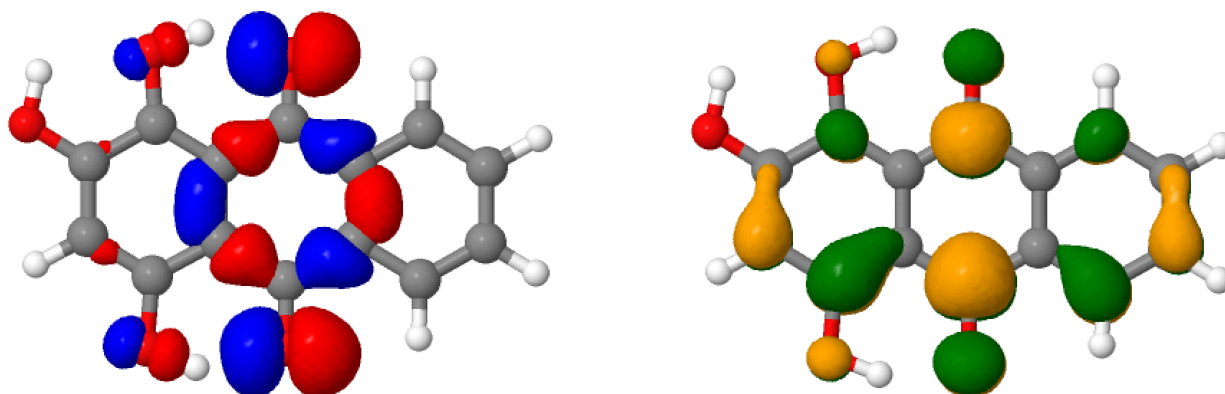


Figure S7: NTOs of $S_0 \rightarrow S_1$ electronic transition: hole(left)/electron(right) orbitals.

4 Investigating the hypothesis of intensity borrowing in the 9,10-anthraquinone and alizarin vibrationally-resolved absorption spectrum

As mentioned in the main text, the similar character ($\pi \rightarrow \pi^*$) of the 9,10-anthraquinone S_3 , S_4 , S_5 and S_6 excited states may suggest the possibility of intensity borrowing from the bright dipole-allowed transitions (S_4 and S_6) to the dark dipole-forbidden ones (S_3 and S_5). This mechanism, which cannot be represented by the Herzberg-Teller (HT) correction to the transition dipole moment, is triggered by non-adiabatic couplings between electronic adiabatic states [D. Aranda and F. Santoro, Journal of Chemical Theory and Computation, 2021, 17, 1691–1700.]

The plot of the excitation energy curves around the S_5 minimum-energy structure, following the 58th normal mode suggested by the HT calculation is reported in Figure S8.

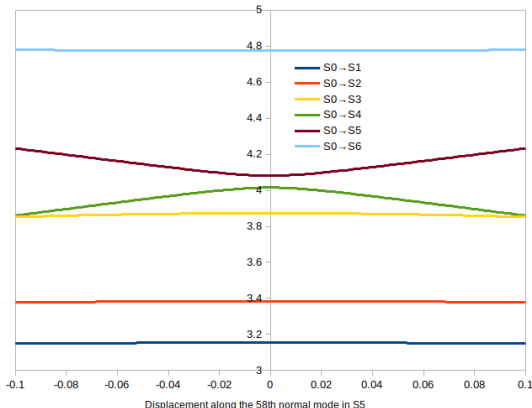


Figure S8: $S_0 \rightarrow S_1$ to $S_0 \rightarrow S_6$ excitation energies (in eV) when the geometry changes from the S_5 minimum-energy structure ($x = 0$), following the S_5 normal mode 58.

In the \mathcal{D}_{2h} point group, coupling between the S_5 and S_6 states is possible via the b_{1u} vibrational modes, which act as coupling modes. Along these type of modes, the point group is lowered to \mathcal{C}_{2v} . Unlike in \mathcal{D}_{2h} , in which $S_0 \rightarrow S_5$ was dipole forbidden, in the subgroup both $S_0 \rightarrow S_5$ and $S_0 \rightarrow S_6$ transitions are dipole allowed and of A_1 symmetry. For 9,10-anthraquinone, we extracted the linear interstate vibronic couplings via fitting of 1D potential energy cuts along b_{1u} modes (see Fig. S9). The modes used for this expansion were those of S_0 , which was taken as reference. The interstate coupling between these two states is negligible (less than 10^{-6} eV) in all cases. This is a consequence of the large gap (around 0.6 eV) between S_5 and S_6 states at the FC region, which does not show any apparent avoided crossing between the surfaces. Therefore, the mechanism of intensity borrowing between S_5 and S_6 can be completely excluded.

A different story happens between S_4 and S_5 , in which the energetic gap is around 0.1 eV, and could therefore be an intensity borrowing mechanism. The coupling modes in this case are b_{2u} vibrational modes, which lower the \mathcal{D}_{2h} point group also to \mathcal{C}_{2v} . Similar than the previous case, both $S_0 \rightarrow S_4$ and $S_0 \rightarrow S_5$ become dipole-allowed transitions of A_1 symmetry. We extracted the linear interstate vibronic couplings via fitting of 1D potential energy cuts along b_{2u} modes (see Fig. S10). Three modes lead to an important vibronic coupling, namely mode 17 with a coupling value of 0.027 eV, mode 30 and mode 53, both with a value of 0.035 eV. The rest of couplings are negligible. This potentially opens the possibility of an efficient population transfer between S_4 to S_5 . An efficient transfer between the two states would lead to an intensity borrowing mechanism, in which the bright S_4 would lose some intensity in favor of the S_5 . For testing this idea, we have created a simple linear vibronic coupling model for S_4 and S_5 along the three b_{2u} modes showing an important interstate vibronic coupling. Along with the interstate couplings, we have added the linear and quadratic potentials in the diagonal diabatic energies taken from S_0 . The linear terms are ± 0.003 eV for S_4 and S_5 along mode 17, ± 0.015 along mode 30 and ± 0.008 eV along mode 53. The quadratic terms are 0.019 eV for S_4 and 0.018 eV for S_5 along mode 17, 0.031 eV and 0.029 eV for mode 30 and 0.052 eV for S_4 and 0.035 eV for S_5 along mode 53. We have subsequently performed an MCTDH propagation on the S_4 state. In Fig. S11, the diabatic population of S_4 stays above 95% all along the dynamics and, consequently, the population of S_5 only acquires 5%. Therefore, we can conclude that intensity-borrowing mechanism contribution to the S_5 intensity is negligible, and therefore the intensity of S_5 comes rather from the symmetry lowering $\mathcal{D}_{2h} \rightarrow \mathcal{C}_{2v}$ which makes this state bright as described by the HT correction.

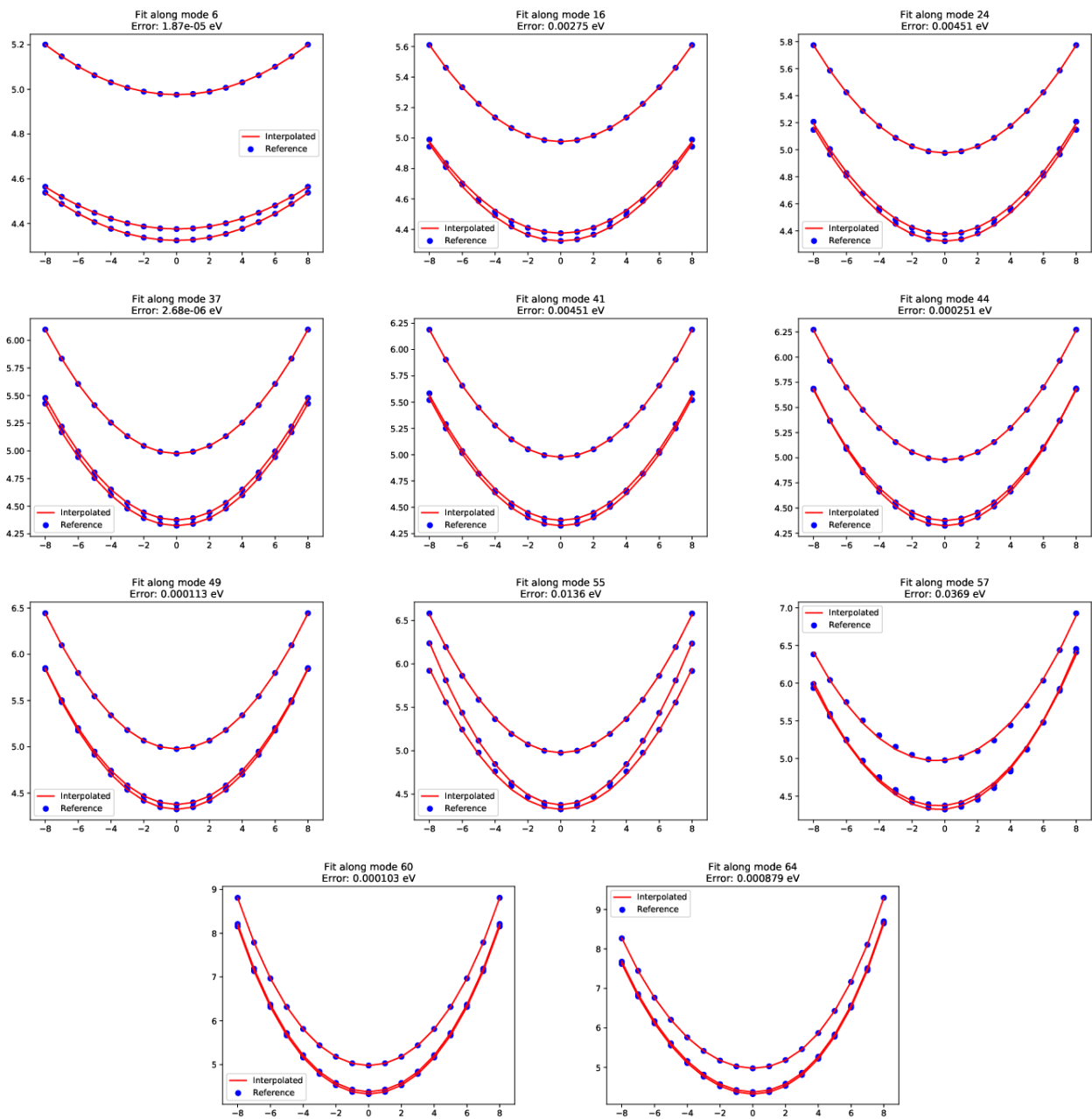


Figure S9: Potential energy surface cuts along b_{1u} modes of 9,10-anthraquinone at the S_0 minimum.

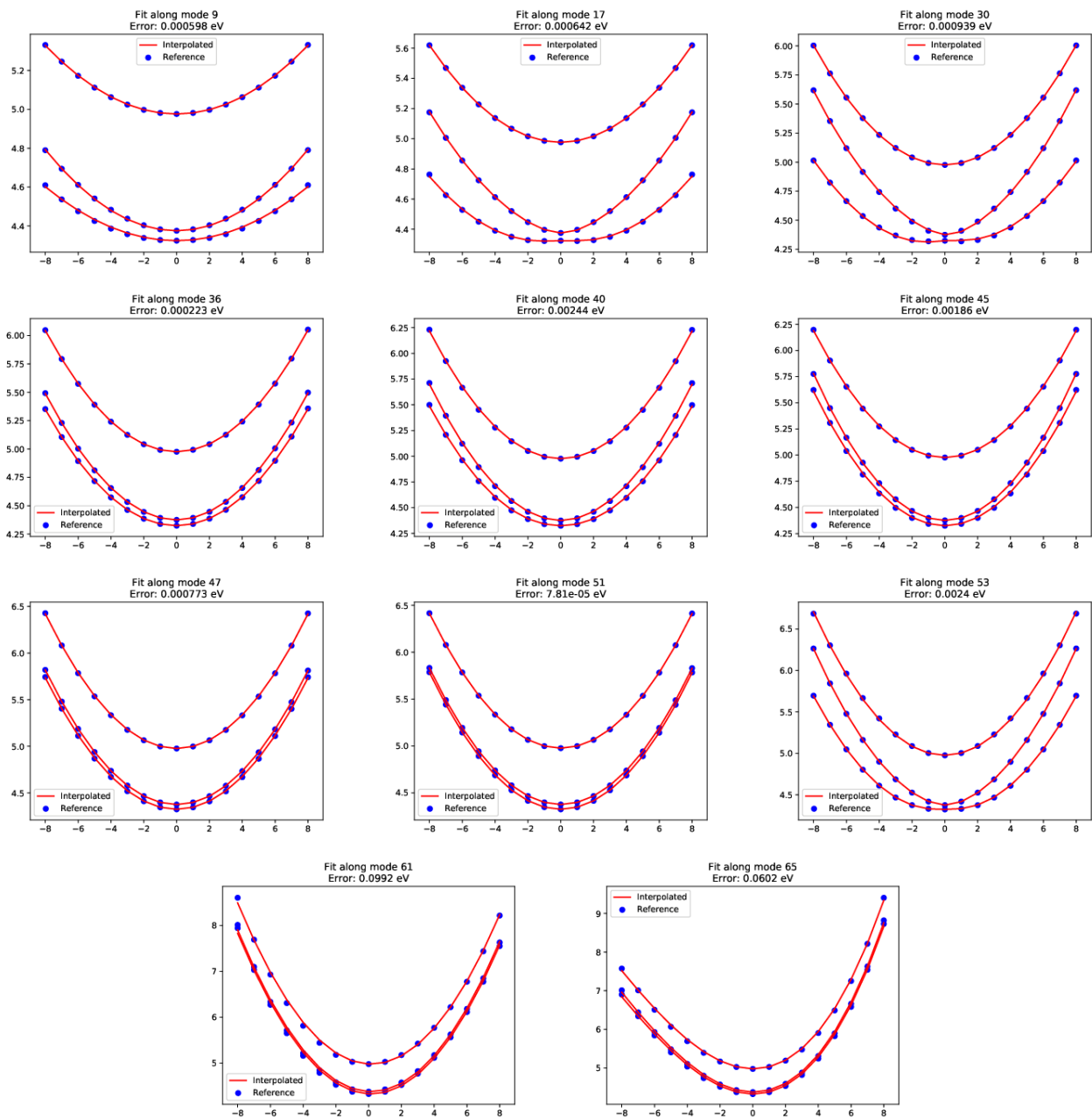


Figure S10: Potential energy surface cuts along b_{2u} modes of 9,10-anthraquinone at the S_0 minimum.

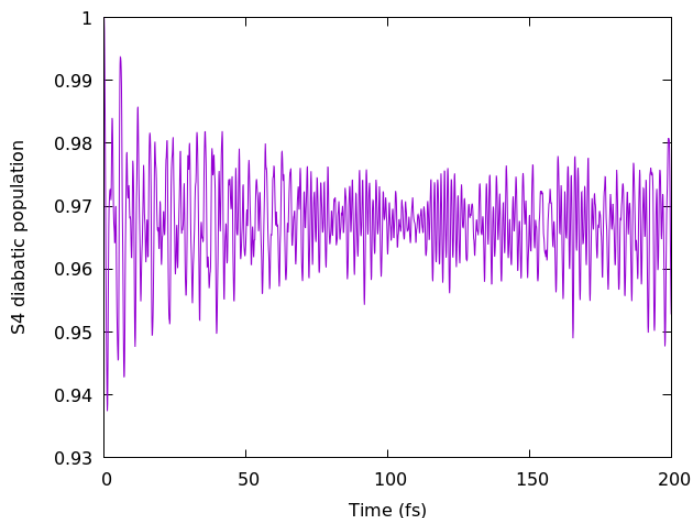


Figure S11: Evolution of the S_4 diabatic population in a linear vibronic coupling model of S_4 and S_5 expanded in the coupling modes 17, 30 and 53 of b_{2u} symmetry.

The same question regarding intensity borrowing occurs in the case of alizarin: its S_1 and S_2 states are energetically very close and may interact non-adiabatically. We have followed the same procedure as we did with 9,10-anthraquinone. As a first step, transition energies have been plotted against geometrical modifications following the normal modes identified as the ones responsible for the triggering of the $n \rightarrow \pi^*$ transition (Figure S12).

The quasi-degeneracy between the S_1 and S_2 states is preserved, whatever the displacement. Qualitatively, the energy profiles don't reveal the presence of important non-adiabatic couplings. Nevertheless, since coupling between the alizarin excited states may occur through a'' modes, we have also built a LVC model hamiltonian using S_0 energy cuts along 23 normal modes. As it can be evidenced in Figures S13 and S14, S_1 and S_2 states don't non-adiabatically interact while they are always energetically close. Accordingly, intensity borrowing does not play a significant role in the alizarin absorption spectrum.

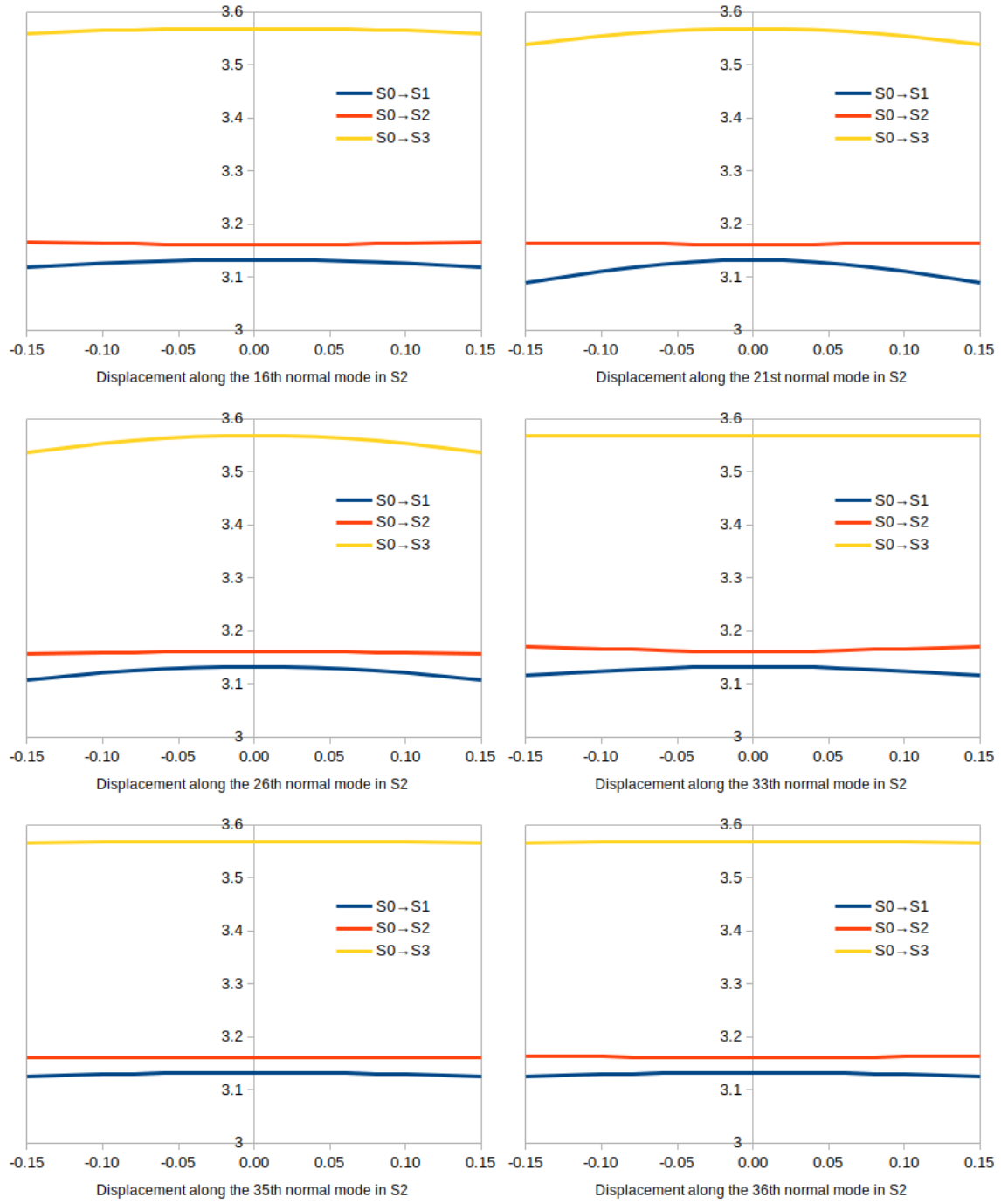


Figure S12: $S_0 \rightarrow S_1$, $S_0 \rightarrow S_2$ and $S_0 \rightarrow S_2$ excitation energies (in eV) when the geometry changes from the S_2 minimum-energy structure ($x = 0$), following the S_2 normal modes 16, 21, 26, 33, 35 and 36.

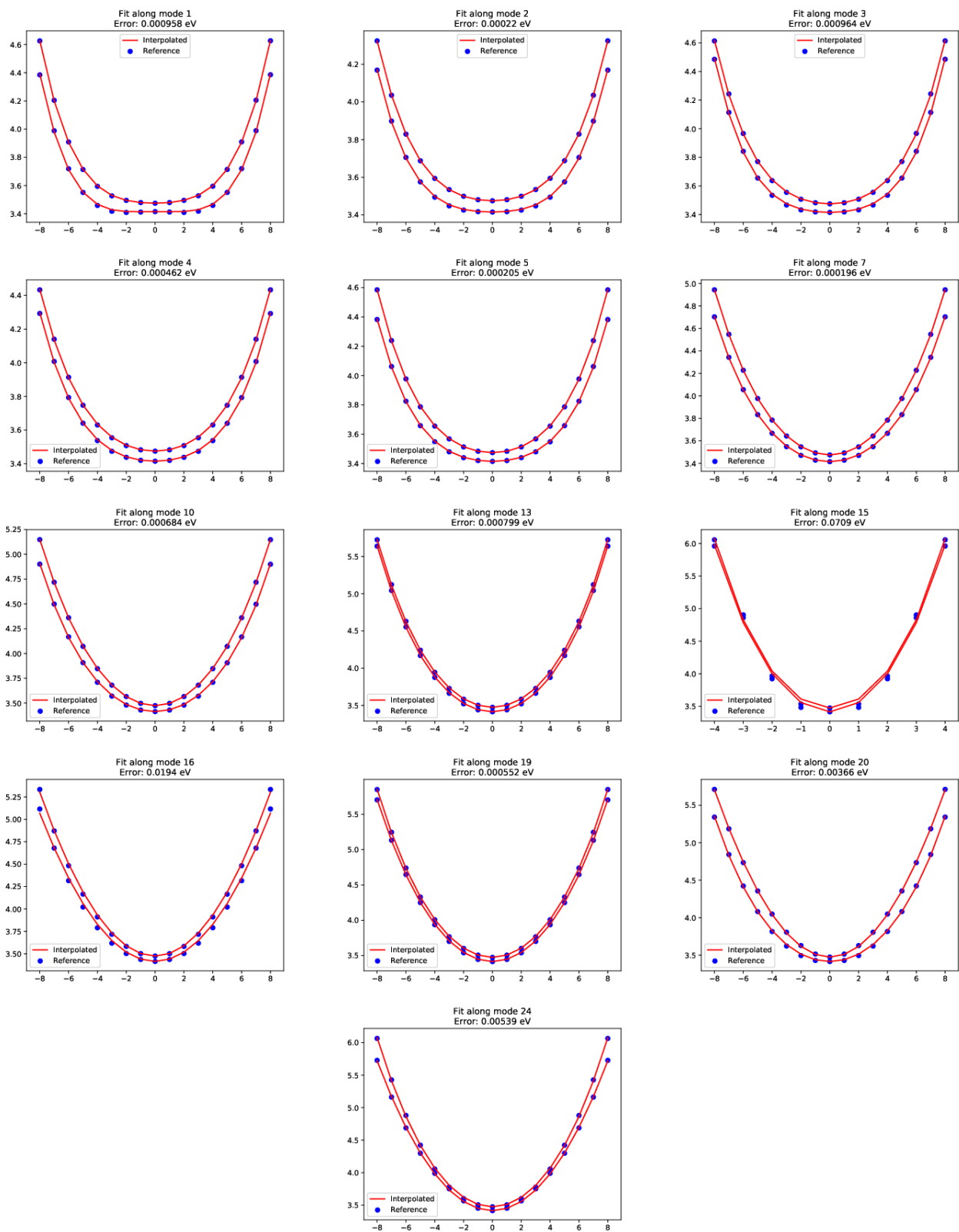


Figure S13: Potential energy surface cuts along a'' modes of alizarin at the S_0 minimum.

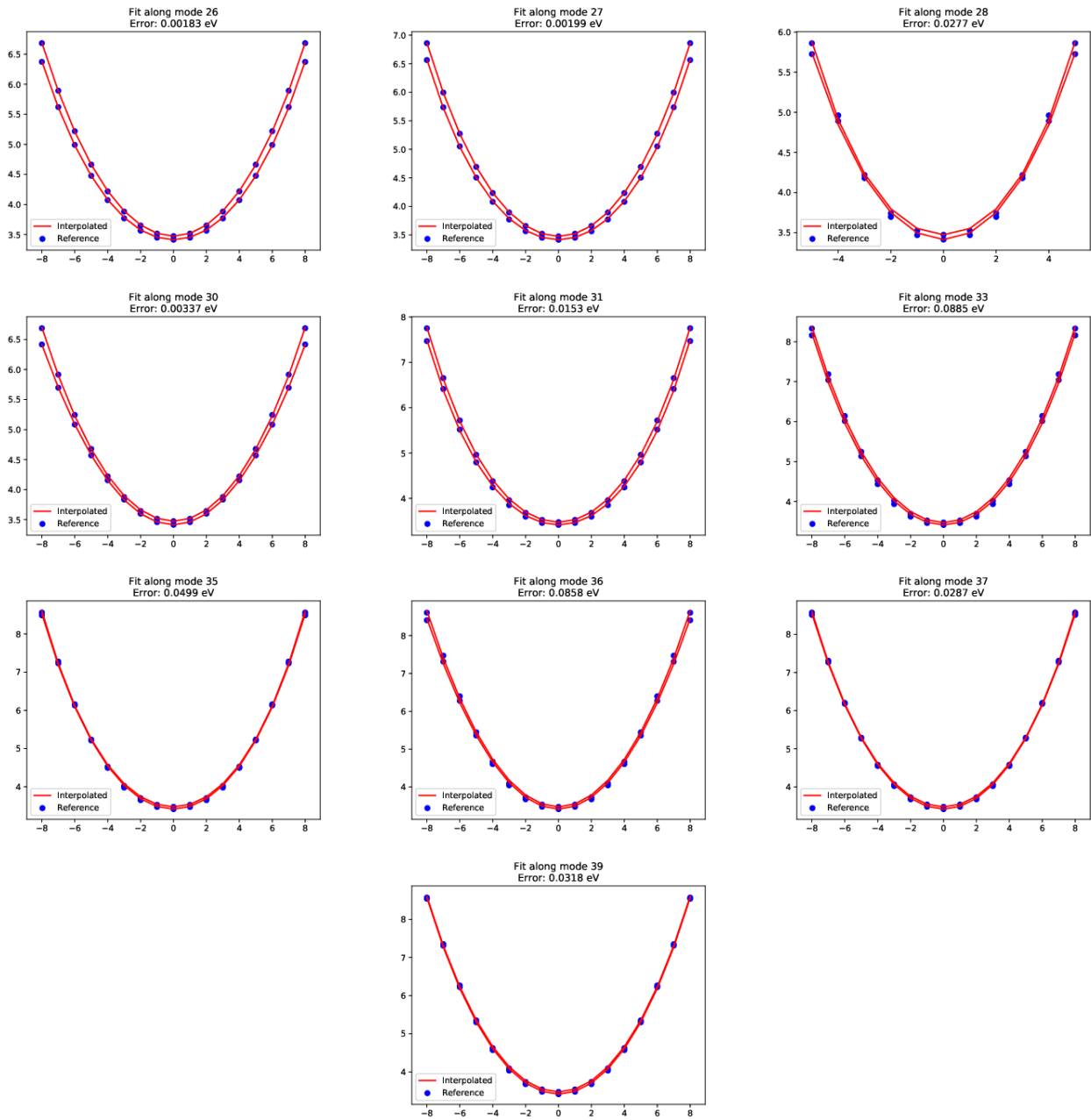


Figure S14: (continue) figure S13

5 Identification of the impurity present in the purpurin solution

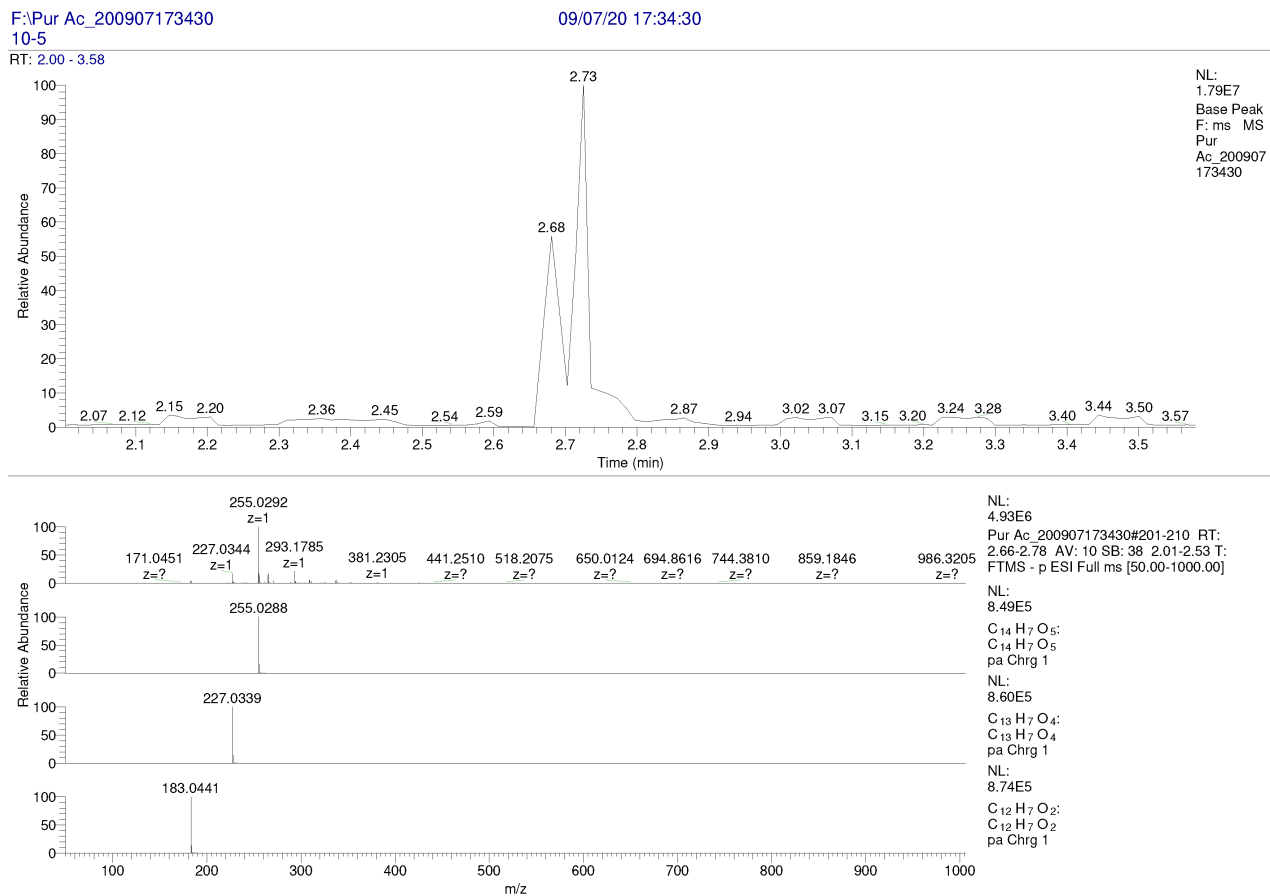


Figure S15: Purpurin Electrospray ionization mass spectrum.

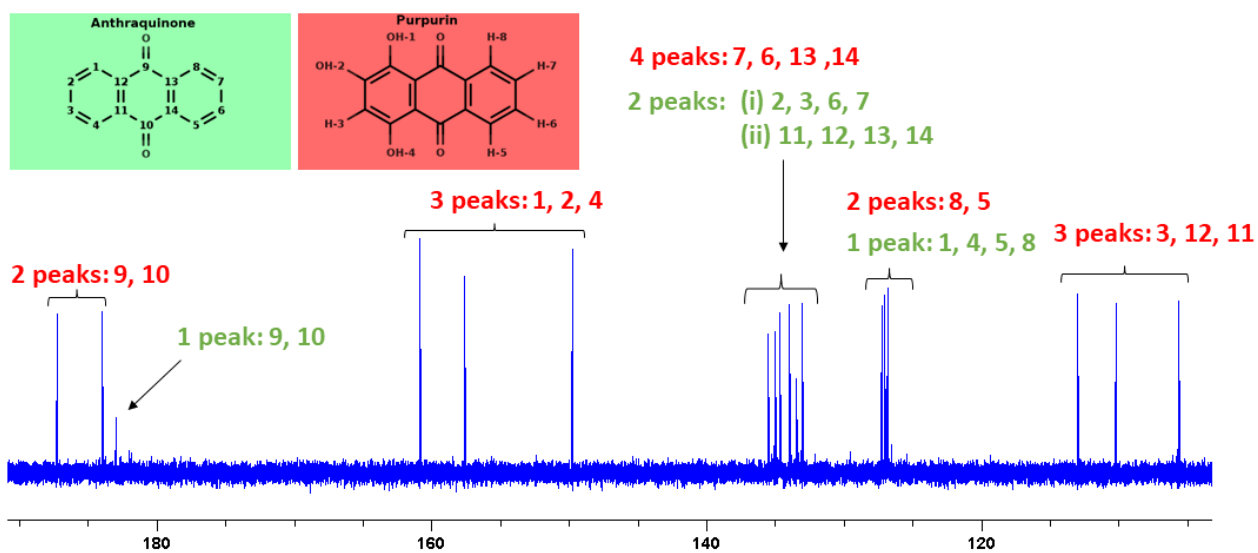


Figure S16: ^{13}C -NMR spectrum of purpurin (red) in $\text{DMSO-}d_6$ (chemical shift in ppm) at room temperature. It confirms the presence of significant amounts of 9,10-anthraquinone (green).